Acta Crystallographica Section C
Crystal Structure Communications
ISSN 0108-2701

2,5-Diaryl-1,3,4-selenadiazoles prepared from Woollins' reagent

David B. Cordes, Guoxiong Hua, Alexandra M. Z. Slawin and J. Derek Woollins*

School of Chemistry, University of St Andrews, Fife KY16 9ST, Scotland
Correspondence e-mail: jdw3@st-andrews.ac.uk

Received 28 September 2011
Accepted 21 November 2011
Online 26 November 2011

Two polymorphs of 2,5-diphenyl-1,3,4-selenadiazole, $C_{14}H_{10}N_2Se$, denoted (I*a*) and (I*b*), and a new polymorph of 2,5-bis(thiophen-2-yl)-1,3,4-selenadiazole, $C_{10}H_6N_2S_2Se$, (II*b*), form on crystallization of the compounds, prepared using Woollins' reagent (2,4-diphenyl-1,3-diselenadiphosphetane 2,4-diselenide). These compounds, along with 2-(4-chlorophenyl)-5-phenyl-1,3,4-selenadiazole, $C_{14}H_9ClN_2Se$, (III), and 2-(furan-2-yl)-5-(*p*-tolyl)-1,3,4-selenadiazole, $C_{13}H_{10}N_2OSe$, (IV), show similar intermolecular interactions, with π–π stacking, C—H$\cdots\pi$ interactions and weak hydrogen bonds typically giving rise to molecular chains. However, the combination of interactions differs in each case, giving rise to different packing arrangements. In polymorph (I*b*), the molecule lies across a crystallographic twofold rotation axis, and (IV) has two independent molecules in the asymmetric unit.

Comment

Interest in using organoselenium heterocycles as compounds with novel properties has expanded rapidly during the last three decades. This interest has focused on areas as diverse as pharmaceutically interesting compounds (Klayman & Gunther, 1973; Mugesh *et al.*, 2001; Nicolaou & Petasis, 1984) and new reagents with unusual reactivity profiles (Back, 2000; Wirth, 2000*a*,*b*). The selenation reagent 2,4-diphenyl-1,3-diselenadiphosphetane 2,4-diselenide, $[PhP(Se)(\mu\text{-}Se)]_2$, known as Woollins' reagent, is the selenium counterpart of the well known Lawesson's reagent. It has been shown to insert selenium into a wide range of different compounds, including in the formation of the title 2,5-diaryl-1,3,4-selenadiazoles (for examples, see Hua *et al.*, 2009; Hua, Cordes *et al.* 2011; Hua, Griffin *et al.*, 2011, and references therein). Five crystal structures have been determined for four selenadiazoles, two of which are polymorphs of each other, and another of which is a polymorph of a known structure; these are 2,5-diphenyl-1,3,4-selenadiazole, (I*a*) (Fig. 1) and (I*b*) (Fig. 2), 2,5-bis(thiophen-2-yl)-1,3,4-selenadiazole, (II*b*) (Fig. 3), 2-(4-chlorophenyl)-5-phenyl-1,3,4-selenadiazole, (III) (Fig. 4), and 2-(furan-2-yl)-5-(*p*-tolyl)-1,3,4-selenadiazole, (IV) (Fig. 5). All five compounds were prepared according to published methods (Hua *et al.*, 2009; Hua, Cordes *et al.*, 2011), and crystals were grown in each case by the diffusion of hexane into a dichloromethane solution of the compound.

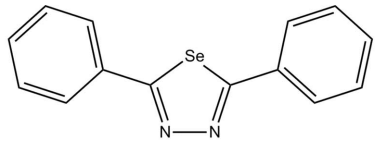

(I*a*)/(I*b*)

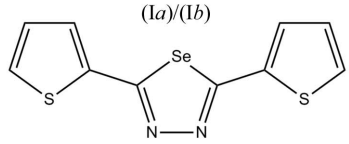

(II*b*)

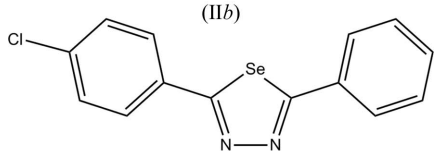

(III)

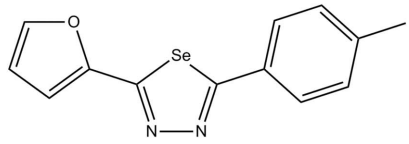

(IV)

Three of the five structures have a single molecule of the compound in the asymmetric unit, the exceptions being polymorph (I*b*) and compound (IV). In (I*b*), the asymmetric unit comprises half a molecule of 2,5-diphenyl-1,3,4-selenadiazole, the other half being generated by twofold rotational symmetry, whereas in (IV), two independent molecules of

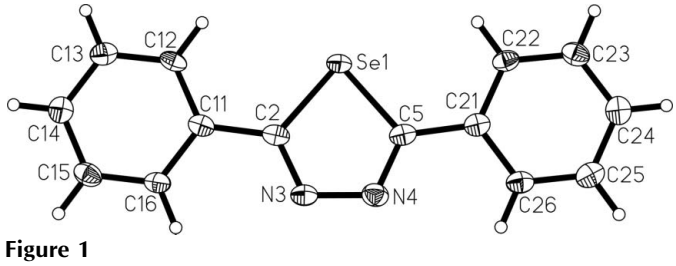

Figure 1
The molecular structure of polymorph (I*a*), with displacement ellipsoids drawn at the 50% probability level.

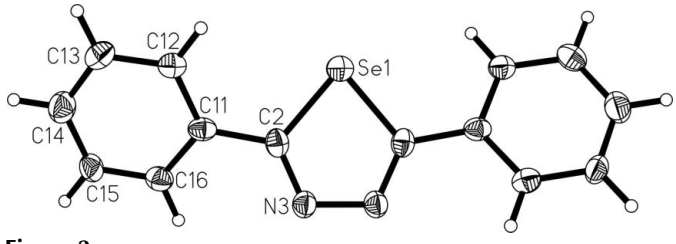

Figure 2
The molecular structure of polymorph (I*b*), with displacement ellipsoids drawn at the 50% probability level. Only the asymmetric unit of the structure is labelled (symmetry code to generate the rest of the molecule: $-x, y, -z+\frac{3}{2}$).

 doi:10.1107/S0108270111049900

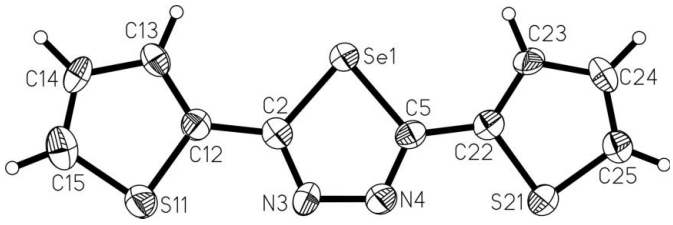

Figure 3
The molecular structure of polymorph (II*b*), with displacement ellipsoids drawn at the 50% probability level.

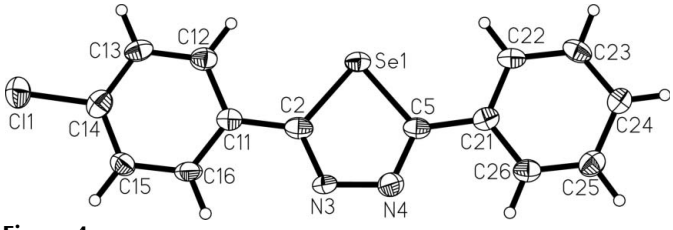

Figure 4
The molecular structure of (III), with displacement ellipsoids drawn at the 50% probability level.

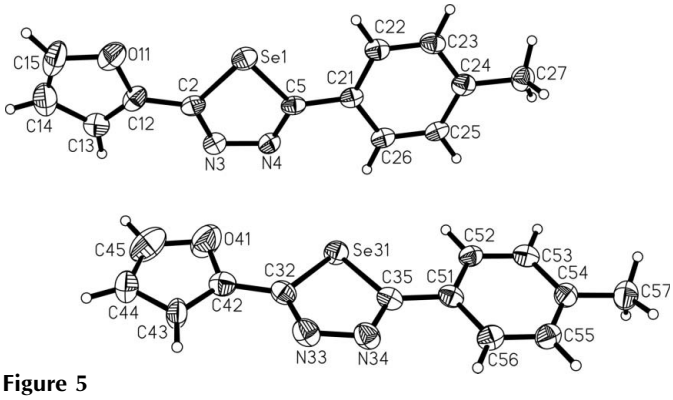

Figure 5
The structure of (IV), with displacement ellipsoids drawn at the 50% probability level.

2-(furan-2-yl)-5-(*p*-tolyl)-1,3,4-selenadiazole form the asymmetric unit. The C—Se bond distances in (I)–(IV) vary from 1.861 (7) to 1.890 (4) Å, falling within the range of C—Se bond lengths seen in selenadiazoles (1.86–1.90 Å; Hua *et al.*, 2009; Hua, Cordes *et al.*, 2011). These distances are shorter than would be expected for a C—Se single bond (*ca* 1.94 Å), indicating that some degree of delocalization occurs. Four of the five structures [excluding (I*b*)] show the same near-planar molecular arrangement seen in previous selenadiazole structures (Hua *et al.*, 2009; Hua, Cordes *et al.*, 2011). The dihedral angles between peripheral ring planes and the selenadiazole rings range from 1.7 (4) to 13.5 (3)°, with the exception of polymorph (I*b*), where the dihedral angle is 22.3 (2)°. Due to its rotational symmetry, this leads to the planes of its phenyl rings being inclined at 43.44 (17)° with respect to each other.

The predominant types of intermolecular interactions in these compounds are those involving their π-systems. All five of the structures show π–π stacking interactions, at a variety of centroid–centroid (*Cg*···*Cg*) distances. While some of these, with *Cg*···*Cg* distances in the range 3.6197 (19)–3.670 (4) Å, fall within the conventional range for π–π interactions, some show apparent π-stacking at distances as long as 3.930 (3) Å (Table 3). While π-interactions at such distances would conventionally be considered insignificant, in these cases the interactions are supported by acting in parallel with other interactions, including other π–π interactions and also C—H···π interactions (see below). All of the compounds, except for (II*b*), also show C—H···π interactions, with C—H···*Cg* distances ranging from 2.52 to 2.97 Å (Table 4). While these longer distances would give rise to very weak interactions, due to their occurring at the conventional van der Waals limit, C—H···π interactions have been suggested to be effective at distances beyond this value (Nishio, 2004). In polymorph (I*b*)

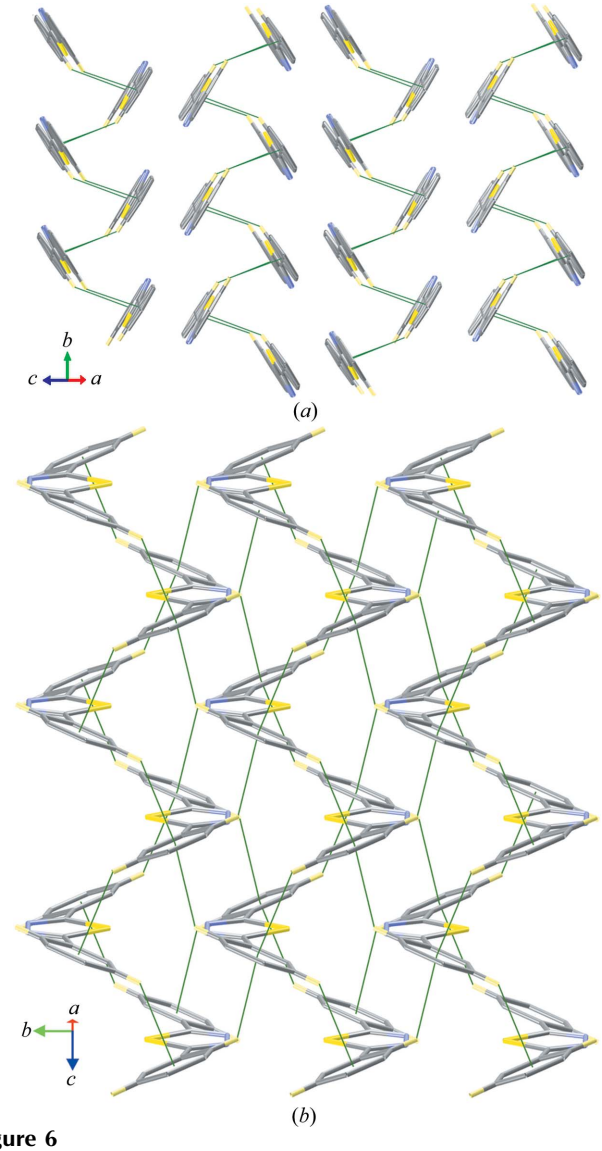

Figure 6
Views of the different two-dimensional sheets in the (100) plane formed by the two polymorphs of (I). C—H···π interactions are shown as thin lines and H atoms not involved in these interactions have been omitted. (*a*) In polymorph (I*a*), chains running along the *b* axis, formed by C—H···π interactions, are linked together by the formation of π-stacked dimers. (*b*) In polymorph (I*b*), two sets of chains, both running along the *c* axis, one formed by π-stacking and C—H···π interactions and the other by different C—H···π interactions, are mutually interconnected.

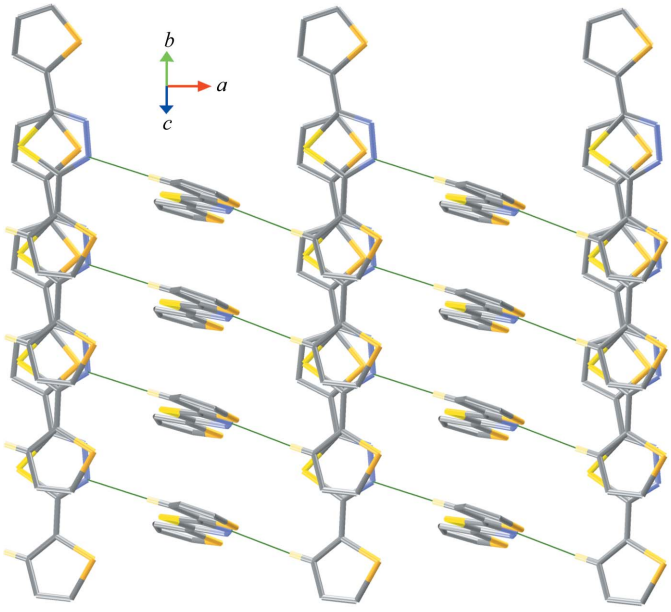

Figure 7
A view of the two-dimensional sheet in the (001) plane in (II*b*), formed by the combination of C—H···N hydrogen bonding and π-stacking. C—H···N hydrogen bonds are shown as thin lines and H atoms not involved in these interactions have been omitted.

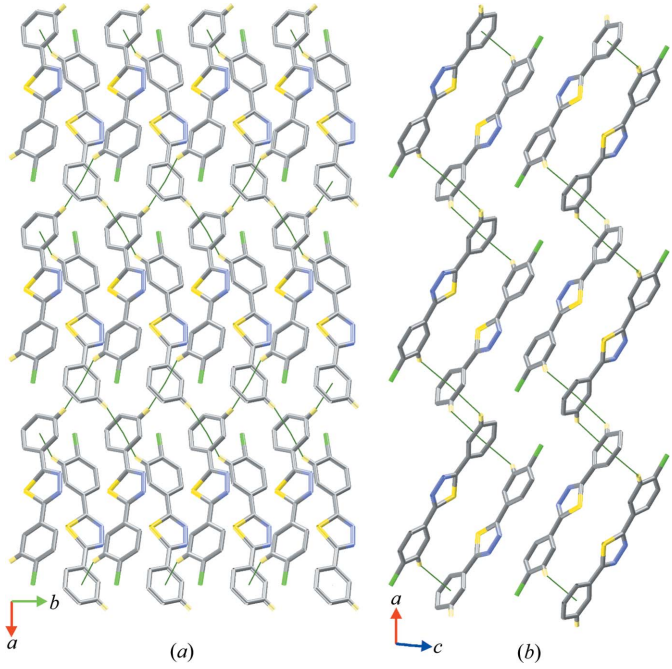

Figure 8
Views of the three-dimensional network which makes up the structure of (III). C—H···π interactions are shown as thin lines and H atoms not involved in these interactions have been omitted. (*a*) The two-dimensional sheet lying in the (001) plane, formed by two sets of C—H···π interactions. (*b*) Two adjacent sheets, showing the π-stacking which connects them into a three-dimensional network.

and in (IV), these interactions occur in conjunction with π–π interactions, mutually reinforcing each other, as in these two compounds there is either sufficient angularity between the phenyl and selenadiazole rings [in (I*b*)] or the presence of the tolyl methyl group [in (IV)] to allow for both C—H···π and π–π interactions between the same adjacent molecules. Further intramolecular interactions occur in (II*b*) and (IV), where weak C—H···N hydrogen bonds contribute to the observed packing motif. These occur at H···N distances of 2.59 Å in (II*b*) and 2.50 and 2.59 Å in (IV), with C···N separations of 3.539 (12), 3.422 (7) and 3.457 (8) Å, respectively.

While this similarity of molecular geometries and types of intramolecular interactions might suggest that similar packing modes would be observed, this is not found to be the case. The intermolecular interactions observed, namely π–π interactions, C—H···π interactions and weak C—H···N hydrogen bonds, combine in different ways, giving rise to a variety of packing motifs. In (I*a*) (Fig. 6), chains formed by C—H···π interactions run along the *b* axis. These interact with adjacent chains by the formation of π-stacked dimers, giving rise to sheets in the (100) plane. In the cases of (I*b*) (Fig. 6) and (II*b*) (Fig. 7), both display two-dimensional sheets formed by the interaction of two different types of chains. Both show π-stacked chains, running along *c* in (I*b*) and along *b* in (II*b*), but the second type of chain is formed by C—H···π interactions along the *c* axis in (I*b*) and by weak hydrogen bonds along the *a* axis in (II*b*), and the resulting sheets occur in the (100) and (001) planes, respectively. The situation in (III) and (IV) is somewhat different, as each comprises a three-dimensional network formed by the linking together of two-dimensional sheets. In (III), two-dimensional sheets are formed in the (001) plane by C—H···π interactions (Fig. 8), whereas in (IV), sheets in the (100) plane are formed by a combination of C—H···π and π–π interactions and C—H···N hydrogen bonding (Fig. 9). In both compounds, these sheets are then linked together into a three-dimensional network by the formation of π-stacked dimers between sheets.

For 2,5-diphenyl-1,3,4-selenadiazole, (I), two visually similar types of polymorphic crystals form under the same conditions. Both of these display a monoclinic unit cell, with polymorph (I*a*) crystallizing in the space group $P2_1/c$ and polymorph (I*b*) in the space group $C2/c$. On a molecular level, there is one key structural difference between the two forms, which appears to give rise to many of the differences observed in their packing. This is the difference in the dihedral angles between the phenyl rings and the selenadiazole ring, with polymorph (I*a*) showing angles of 3.35 (16) and 4.11 (16)°, whereas polymorph (I*b*) shows symmetry-equivalent dihedral angles of 22.3 (2)°. These differences can be seen to lead directly to differences in the packing (Fig. 6), as the twist of the phenyl rings changes both the distance and angle possible for π–π interactions, inducing a molecular offset from the chain axis in (I*b*), and also makes it possible for both π–π and C—H···π interactions to occur in the same molecular chain.

In the case of (II*b*), the crystals appeared to be slightly visually different to those previously found for (II*a*) (Hua, Cordes *et al.*, 2011), and structure analysis revealed it to be a polymorphic form. Polymorph (II*b*) crystallizes in the orthorhombic space group $Pca2_1$, although with broadly similar

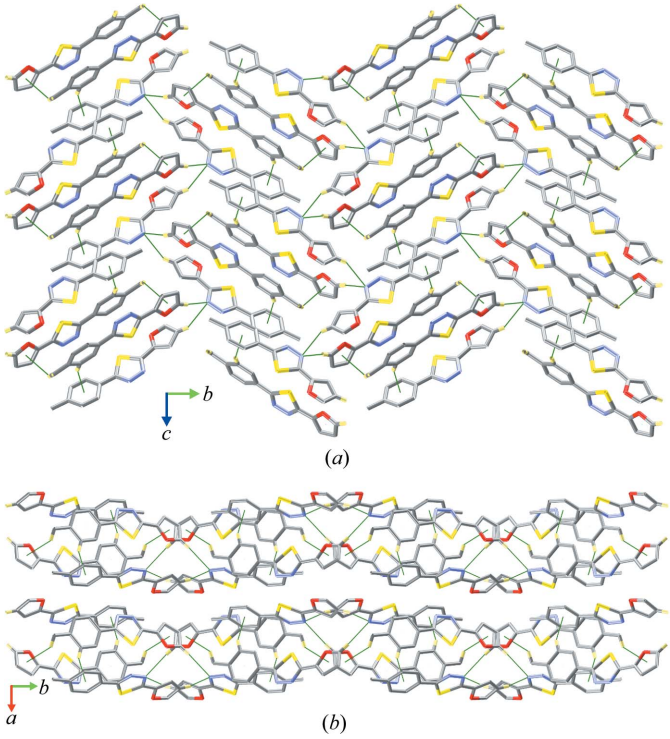

Figure 9
Views of the three-dimensional network which makes up the structure of (IV). C—H···π and C—H···N interactions are shown as thin lines and H atoms not involved in these interactions have been omitted. (*a*) The two-dimensional sheet lying in the (100) plane, formed by the combination of both π-stacking and C—H···π interactions and C—H···N hydrogen bonds. (*b*) Two adjacent sheets, showing the π-stacking which connects them into a three-dimensional network.

unit-cell parameters to the known structure, which crystallizes in the monoclinic space group $P2_1/c$. There is little on a gross structural level to indicate why a different polymorphic form occurs, a fit of all non-H atoms of polymorph (II*b*) to those of polymorph (II*a*) having an r.m.s. deviation of 0.052 Å. Additionally, there are similarities in the packing of the two polymorphs, but the differences between them do become more apparent as the interactions which give rise to the packing are considered. Both polymorphs display π-stacked chains running along the *b* axis, but these are assembled differently. In (II*b*), the π-overlaps occur between the selenadiazole ring and both thiophene rings, whereas in (II*a*) two different sets of π-interactions give rise to a more zigzag chain. Furthermore, (II*b*) also shows chains running along the *a* axis formed by weak C—H···N hydrogen bonding, the combination of these two sets of interactions giving rise to sheets in the (001) plane, while (II*a*) shows no other intermolecular interactions.

Experimental

All compounds were prepared according to literature methods by the reaction of Woollins' reagent with either the appropriate 1,2-diacylhydrazine [for (I*a*), (I*b*), (III) and (IV); Hua *et al.*, 2009] or acylcarbohydrazide [for (II*b*); Hua, Cordes *et al.*, 2011]. X-ray quality crystals of all compounds were grown by the diffusion of hexane into a dichloromethane solution of the compound. Crystals of the two polymorphic forms of 2,5-diphenyl-1,3,4-selenadiazole, *viz.* (I*a*) and (I*b*), were difficult to differentiate visually, except that the platelets of (I*a*) tended to be thicker than those of (I*b*). Crystals of (II*b*) were likewise difficult to differentiate from those of the known polymorph (II*a*) (Hua, Cordes *et al.*, 2011), although those of (II*b*) did tend to display a more intense orange colour.

Polymorph (I*a*)

Crystal data

$C_{14}H_{10}N_2Se$
M_r = 285.20
Monoclinic, $P2_1/c$
a = 13.036 (4) Å
b = 5.4650 (14) Å
c = 16.274 (5) Å
β = 101.860 (7)°
V = 1134.6 (5) Å^3
Z = 4
Mo $K\alpha$ radiation
μ = 3.29 mm^{-1}
T = 93 K
0.15 × 0.10 × 0.05 mm

Data collection

Rigaku Mercury CCD area-detector diffractometer
Absorption correction: multi-scan (*CrystalClear*; Rigaku, 2010)
T_{min} = 0.795, T_{max} = 1.000
7425 measured reflections
2413 independent reflections
2081 reflections with $I > 2\sigma(I)$
R_{int} = 0.037

Refinement

$R[F^2 > 2\sigma(F^2)]$ = 0.041
$wR(F^2)$ = 0.081
S = 1.09
2413 reflections
155 parameters
H-atom parameters constrained
$\Delta\rho_{max}$ = 1.25 e Å^{-3}
$\Delta\rho_{min}$ = −0.69 e Å^{-3}

Polymorph (I*b*)

Crystal data

$C_{14}H_{10}N_2Se$
M_r = 285.20
Monoclinic, $C2/c$
a = 26.763 (10) Å
b = 5.796 (2) Å
c = 7.213 (3) Å
β = 103.885 (9)°
V = 1086.2 (7) Å^3
Z = 4
Mo $K\alpha$ radiation
μ = 3.43 mm^{-1}
T = 93 K
0.25 × 0.20 × 0.01 mm

Data collection

Rigaku Mercury CCD area-detector diffractometer
Absorption correction: multi-scan (*CrystalClear*; Rigaku, 2010)
T_{min} = 0.490, T_{max} = 1.000
3541 measured reflections
1149 independent reflections
1014 reflections with $I > 2\sigma(I)$
R_{int} = 0.053

Refinement

$R[F^2 > 2\sigma(F^2)]$ = 0.066
$wR(F^2)$ = 0.167
S = 1.11
1149 reflections
78 parameters
H-atom parameters constrained
$\Delta\rho_{max}$ = 0.92 e Å^{-3}
$\Delta\rho_{min}$ = −1.14 e Å^{-3}

Polymorph (II*b*)

Crystal data

$C_{10}H_6N_2S_2Se$
M_r = 297.25
Orthorhombic, $Pca2_1$
a = 10.641 (5) Å
b = 5.134 (2) Å
c = 19.096 (8) Å
V = 1043.4 (7) Å^3
Z = 4
Mo $K\alpha$ radiation
μ = 3.96 mm^{-1}
T = 93 K
0.25 × 0.08 × 0.08 mm

Table 1
Hydrogen-bond geometry (Å, °) for (II*b*).

D—H···A	D—H	H···A	D···A	D—H···A
C23—H23···N4^{i}	0.95	2.59	3.539 (12)	177

Symmetry code: (i) $x-\frac{1}{2}, -y+1, z$.

Data collection

Rigaku Mercury CCD area-detector diffractometer
Absorption correction: multi-scan (*CrystalClear*; Rigaku, 2010)
T_{min} = 0.551, T_{max} = 1.000
6487 measured reflections
2060 independent reflections
1704 reflections with $I > 2\sigma(I)$
R_{int} = 0.083

Refinement

$R[F^2 > 2\sigma(F^2)]$ = 0.054
$wR(F^2)$ = 0.116
S = 1.12
2060 reflections
138 parameters
1 restraint
H-atom parameters constrained
$\Delta\rho_{max}$ = 1.08 e Å^{-3}
$\Delta\rho_{min}$ = −0.67 e Å^{-3}
Absolute structure: Flack (1983), with 874 Friedel pairs
Flack parameter: 0.377 (19)

Compound (III)

Crystal data

$C_{14}H_9ClN_2Se$
M_r = 319.64
Monoclinic, $P2_1/c$
a = 13.382 (5) Å
b = 5.5247 (18) Å
c = 16.524 (5) Å
β = 94.528 (8)°
V = 1217.9 (7) Å^3
Z = 4
Mo $K\alpha$ radiation
μ = 3.28 mm^{-1}
T = 93 K
0.12 × 0.07 × 0.01 mm

Data collection

Rigaku Mercury CCD area-detector diffractometer
Absorption correction: multi-scan (*CrystalClear*; Rigaku, 2010)
T_{min} = 0.500, T_{max} = 1.000
7679 measured reflections
2513 independent reflections
2050 reflections with $I > 2\sigma(I)$
R_{int} = 0.058

Refinement

$R[F^2 > 2\sigma(F^2)]$ = 0.079
$wR(F^2)$ = 0.226
S = 1.06
2513 reflections
163 parameters
H-atom parameters constrained
$\Delta\rho_{max}$ = 4.87 e Å^{-3}
$\Delta\rho_{min}$ = −1.07 e Å^{-3}

Compound (IV)

Crystal data

$C_{13}H_{10}N_2OSe$
M_r = 289.19
Monoclinic, $P2_1/c$
a = 8.5036 (15) Å
b = 25.210 (5) Å
c = 11.116 (2) Å
β = 96.814 (5)°
V = 2366.2 (8) Å^3
Z = 8
Mo $K\alpha$ radiation
μ = 3.16 mm^{-1}
T = 93 K
0.30 × 0.20 × 0.04 mm

Table 2
Hydrogen-bond geometry (Å, °) for (IV).

D—H···A	D—H	H···A	D···A	D—H···A
C15—H15···N33^{i}	0.95	2.50	3.441 (7)	172
C44—H44···N33^{ii}	0.95	2.59	3.457 (7)	151

Symmetry codes: (i) $x+1, -y+\frac{3}{2}, z-\frac{1}{2}$; (ii) $x, -y+\frac{3}{2}, z-\frac{1}{2}$.

Data collection

Rigaku Mercury CCD area-detector diffractometer
Absorption correction: multi-scan (*CrystalClear*; Rigaku, 2010)
T_{min} = 0.558, T_{max} = 1.000
15690 measured reflections
4865 independent reflections
3778 reflections with $I > 2\sigma(I)$
R_{int} = 0.055

Refinement

$R[F^2 > 2\sigma(F^2)]$ = 0.057
$wR(F^2)$ = 0.147
S = 1.07
4865 reflections
309 parameters
H-atom parameters constrained
$\Delta\rho_{max}$ = 1.35 e Å^{-3}
$\Delta\rho_{min}$ = −1.03 e Å^{-3}

C-bound H atoms were included in calculated positions (C—H = 0.98 Å for methyl H atoms and 0.95 Å for aryl H atoms) and refined as riding, with U_{iso}(H) = 1.2U_{eq}(C) for aryl or 1.5U_{eq}(C) for methyl H atoms. The structure of (II*b*) shows signs of racemic twinning, the Flack (1983) parameter being 0.377 (19). This is complicated by the Friedel-pair coverage being lower than ideal, at 68%, which suggests that the Flack parameter in this case may be less meaningful than generally. In (III), a difference electron-density feature of 4.87 e Å^{-3} was located 1.37 Å from atom Se1, but this has no chemical significance. This feature possibly arises due to a Fourier ripple, and results in the slightly elevated value of R for this structure. Multiple crystals were tried, the majority of which showed much weaker diffraction at higher angles.

Table 3
Distances of π–π interactions (Å).

*Cg*1 and *Cg*2 are the centroids of the Se1–C5 and C11–C16 rings, respectively, of polymorph (I*a*). *Cg*3 is the centroid of the Se1–C5 ring of polymorph (I*b*). *Cg*4, *Cg*5 and *Cg*6 are the centroids of the Se1–C5, S11–C15 and S21–C25 rings, respectively, of (II*b*). *Cg*7 and *Cg*8 are the centroids of the Se1–C5 and C11–C16 rings, respectively, of (III). *Cg*9, *Cg*10 and *Cg*11 are the centroids of the Se1–C5, C21–C26 and C51–C56 rings, respectively, of (IV).

Compound	Centroids	$Cg\cdots Cg$
(I*a*)	$Cg1\cdots Cg2^{i}$	3.6197 (19)
(I*b*)	$Cg3\cdots Cg3^{ii}$	3.848 (3)
(II*b*)	$Cg4\cdots Cg5^{iii}$	3.636 (4)
	$Cg4\cdots Cg6^{iv}$	3.861 (4)
(III)	$Cg7\cdots Cg8^{v}$	3.670 (4)
(IV)	$Cg9\cdots Cg10^{vi}$	3.930 (3)
	$Cg11\cdots Cg11^{vii}$	3.898 (3)

Symmetry codes: (i) $-x+2, -y, -z+1$; (ii) $-x, -y+1, -z+1$; (iii) $x, y-1, z$; (iv) $x, y+1, z$; (v) $-x+1, -y, -z+1$; (vi) $-x+2, -y+1, -z+1$; (vii) $-x+1, -y+1, -z+1$.

Table 4
Geometry of C—H···π interactions (Å, °).

*Cg*1 and *Cg*2 are the centroids of the C11–C16 and C21–C26 rings, respectively, of polymorph (I*a*). *Cg*3 is the centroid of the C11–C16 ring of polymorph (I*b*). *Cg*4 is the centroid of the C21–C26 ring of (III). *Cg*5 and *Cg*6 are the centroids of the C51–C56 and O11–C15 rings, respectively, of (IV).

Compound	C—H···Cg	H···Cg	C···Cg	C—H···Cg
(I*a*)	C22—H22···$Cg1^{i}$	2.89	3.660 (3)	139
	C13—H13···$Cg2^{i}$	2.97	3.649 (3)	130
(I*b*)	C16—H16···$Cg3^{ii}$	2.81	3.416 (6)	122
	C13—H13···$Cg3^{iii}$	2.94	3.621 (7)	130
(III)	C13—H13···$Cg4^{iv}$	2.77	3.497 (7)	134
	C25—H25···$Cg4^{v}$	2.93	3.673 (7)	136
(IV)	C23—H23···$Cg5^{vi}$	2.52	3.389 (5)	151
	C27—H27*C*···$Cg6^{vii}$	2.89	3.549 (6)	125

Symmetry codes: (i) $-x+2, y+\frac{1}{2}, -z+\frac{1}{2}$; (ii) $x, -y+1, z-\frac{1}{2}$; (iii) $x, -y, z-\frac{1}{2}$; (iv) $-x+1, y+\frac{1}{2}, -z+\frac{3}{2}$; (v) $-x+2, y-\frac{1}{2}, -z+\frac{3}{2}$; (vi) $x+1, y, z$; (vii) $-x+2, -y+1, -z+1$.

For all compounds, data collection: *CrystalClear* (Rigaku, 2010); cell refinement: *CrystalClear*; data reduction: *CrystalClear*; program(s) used to solve structure: *SHELXTL* (Sheldrick, 2008); program(s) used to refine structure: *SHELXTL*; molecular graphics: *SHELXTL* and *OLEX* (Dolomanov *et al.*, 2003); software used to prepare material for publication: *SHELXTL*, *PLATON* (Spek, 2009) and *publCIF* (Westrip, 2010).

The authors are grateful to the University of St Andrews and the Engineering and Physical Science Research Council (EPSRC, UK) for financial support.

Supplementary data for this paper are available from the IUCr electronic archives (Reference: BM3112). Services for accessing these data are described at the back of the journal.

References

Back, T. G. (2000). *Organoselenium Chemistry: A Practical Approach*. New York: Oxford University Press Inc.
Dolomanov, O. V., Blake, A. J., Champness, N. R. & Schröder, M. (2003). *J. Appl. Cryst.* **36**, 1283–1284.
Flack, H. D. (1983). *Acta Cryst.* A**39**, 876–881.
Hua, G., Cordes, D. B., Li, Y., Slawin, A. M. Z. & Woollins, J. D. (2011). *Tetrahedron Lett.* **52**, 3311–3314.
Hua, G., Griffin, J. M., Ashbrook, S. E., Slawin, A. M. Z. & Woollins, J. D. (2011). *Angew. Chem. Int. Ed.* **50**, 4123–4126.
Hua, G., Li, Y., Fuller, A. L., Slawin, A. M. Z. & Woollins, J. D. (2009). *Eur. J. Org. Chem.* pp. 1612–1618.
Klayman, D. L. & Gunther, W. H. H. (1973). Editors. *Organic Selenium Compounds: Their Chemistry and Biology*. New York: Wiley.
Mugesh, G., Du Mont, W. W. & Sies, H. (2001). *Chem. Rev.* **101**, 2125–2179.
Nicolaou, K. C. & Petasis, N. A. (1984). *Selenium in Natural Products Synthesis*. Philadelphia: CIS.
Nishio, M. (2004). *CrystEngComm*, **6**, 130–158.
Rigaku (2010). *CrystalClear*. Version 2.0. Rigaku Americas, The Woodlands, Texas, USA, and Rigaku Corporation, Tokyo, Japan.
Sheldrick, G. M. (2008). *Acta Cryst.* A**64**, 112–122.
Spek, A. L. (2009). *Acta Cryst.* D**65**, 148–155.
Westrip, S. P. (2010). *J. Appl. Cryst.* **43**, 920–925.
Wirth, T. (2000*a*). *Angew. Chem. Int. Ed.* **39**, 3740–3749.
Wirth, T. (2000*b*). Editor. *Topics in Current Chemistry: Organoselenium Chemistry, Modern Developments in Organic Synthesis*. Heidelberg: Springer.